IOPscience iopscience.iop.org

Home Search Collections Journals About Contact us My IOPscience

Submolecular resolution in scanning probe images of Sn-phthalocyanines on Cu(100) using metal tips

This content has been downloaded from IOPscience. Please scroll down to see the full text.

2017 J. Phys.: Condens. Matter 29 394004

(http://iopscience.iop.org/0953-8984/29/39/394004)

View the table of contents for this issue, or go to the journal homepage for more

Download details:

IP Address: 145.116.143.12
This content was downloaded on 22/08/2017 at 10:10

Please note that terms and conditions apply.

IOP Publishing Journal of Physics: Condensed Matter
J. Phys.: Condens. Matter **29** (2017) 394004 (5pp) https://doi.org/10.1088/1361-648X/aa7dbd

Submolecular resolution in scanning probe images of Sn-phthalocyanines on Cu(1 0 0) using metal tips

Kristof Buchmann[1], **Nadine Hauptmann**[2], **Adam S Foster**[3,4] **and Richard Berndt**[1]

[1] Institut für Experimentelle und Angewandte Physik, Christian-Albrechts-Universität zu Kiel, D-24098 Kiel, Germany
[2] Institute for Molecules and Materials, Radboud University, 6525 AJ Nijmegen, Netherlands
[3] COMP, Department of Applied Physics, Aalto University, Otakaari 1, FI-00076 Helsinki, Finland
[4] Division of Electrical Engineering and Computer Science, Kanazawa University, Kanazawa 920-1192, Japan

E-mail: n.hauptmann@science.ru.nl and berndt@physik.uni-kiel.de

Received 26 April 2017, revised 3 July 2017
Accepted for publication 5 July 2017
Published 22 August 2017

Abstract

Single Sn-phthalocyanine (SnPc) molecules adsorb on Cu(1 0 0) with the Sn ion above (Sn-up) or below (Sn-down) the molecular plane. Here we use a combination of atomic force microscopy (AFM), scanning tunnelling microscopy (STM) and first principles calculations to understand the adsorption configuration and origin of observed contrast of molecules in the Sn-down state. AFM with metallic tips images the pyrrole nitrogen atoms in these molecules as attractive features while STM reveals a chirality of the electronic structure of the molecules close to the Fermi level E_F, which is not observed in AFM. Using density functional theory calculations, the origin of the submolecular contrast is analysed and, while the electrostatic forces turn out to be negligible, the van der Waals interaction between the phenyl rings of SnPc and the substrate deform the molecule, push the pyrrole nitrogen atoms away from the substrate and thus induce the observed submolecular contrast. Simulated STM images reproduce the chirality of the electronic structure near E_F.

Keywords: atomic force microscopy, density functional theory, Sn-phthalocyanine, scanning tunneling microscopy

(Some figures may appear in colour only in the online journal)

1. Introduction

Over the past decade, combined scanning tunnelling (STM) and atomic force microscopy (AFM) has become increasingly popular as a tool to study molecules on surfaces. STM often provides insight into the energy-resolved electronic structure of the adsorbate [1]. Through Pauli repulsion, AFM tends to be more sensitive to the total electron density, which is linked to the molecular structure [2–5]. In detail, however, image interpretation remains a difficult task [6, 7]. The positions of the atoms of the tip and the molecule may be affected by their mutual interactions to varying degrees [8–11]. In addition, electrostatic forces have to be taken into account, which in turn depend on the largely unknown dipole moment of the tip [12–16]. Accurately treating dispersion interactions adds another degree of complication [17, 18].

Given this state of affairs, it is useful to investigate adsorbed molecules that are simple enough to enable a theoretical treatment and disentangle the relevant forces. Phthalocyanines appear suitable for this purpose. Through variation of the metal ion at their center, the bonding to the substrate and the intramolecular charge transfer can be tuned [19]. In the case of Sn-phthalocyanine on Ag(1 1 1), the presence of two distinct adsorption geometries with the Sn ion above (Sn-up) or

 © 2017 IOP Publishing Ltd Printed in the UK

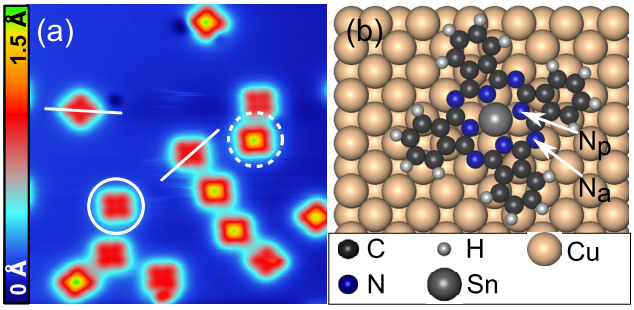

Figure 1. (a) Constant-current STM image of SnPc molecules adsorbed on Cu(1 0 0) ((15 nm)^2, $V = 1$ V; $I = 20$ pA). Sn-down (solid circle) and Sn-up (dashed circle) configurations are readily distinguished by the different apparent height of the molecular center. Two orientations of the molecular lobes (solid lines) are observed. (b) Top-view of a Sn-down molecule on Cu(1 0 0) calculated by DFT. Examples of nitrogen atoms in the pyrrole (N_p) and azopyrrole (N_a) positions are indicated by arrows.

below (Sn-down) the plane of the macrocycle adds an additional twist [20–24]. Here, we focus on SnPc molecules in the Sn-down state on the more reactive Cu(1 0 0) substrate and using combined STM/AFM we observed submolecular contrast. Density functional theory (DFT) calculations are used to analyse its origin and show that the influence of electrostatic forces is negligible here. Rather, the strong interaction between the phenyl rings of SnPc with the surface deforms the molecule. As a result, the pyrrole nitrogen atoms are pushed above the molecular plane, which then leads to the observed submolecular contrast.

2. Methods

The measurements were performed with a combined scanning tunnelling and atomic force microscope in ultra-high vacuum at a temperature of 5 K [25]. Non-contact frequency-modulation mode was utilised for AFM measurements with a Q-plus sensor [26]. The free prong of the quartz tuning fork oscillated with an amplitude of ∼1 Å at its resonance frequency of ∼23 kHz. An etched W tip was attached to the free prong in order to measure the tunnelling current I averaged over the range of the tip oscillation simultaneously with the frequency shift Δf of the tuning fork. The voltage was applied to the sample.

Cu(1 0 0) surfaces were prepared by sputtering and annealing cycles. Sn-phthalocyanine molecules (*Santa Cruz biotechnology*) were sublimated from a molybdenum crucible onto the Cu(1 0 0) with sub-monolayer coverage. The substrate was kept at 20 °C during deposition. W tips were covered with Cu by repeatedly indenting them into the substrate until submolecular resolution in constant current STM mode was achieved.

All first principles calculations were performed using the periodic plane-wave basis code VASP [27, 28] implementing the spin-polarised density functional theory (DFT). To accurately include van der Waals interaction in this system we used the optB86B + vdW–DF functional [29–31], selected based on previous work showing that it provides a sufficiently accurate description for all subsystems involved in the measurement. Projected augmented wave (PAW) potentials were used to describe the core electrons [32], with a kinetic energy cutoff of 280 eV (with PREC = accurate). Systematic k-point convergence was checked for all systems, with sampling chosen according to system size and the Γ point being used for the final production run. This approach converged the total energy of all the systems to the order of meV. The properties of the bulk and surface of Cu and the isolated molecular structure were carefully checked within this methodology, and excellent agreement was achieved with experiments. A Bader charge analysis was used to estimate charge transfer in the simulations [33]. Simulated STM images were generated using the HIVE-STM code [34].

3. Results and discussion

3.1. Adsorption of SnPc on Cu(1 0 0)

A constant current STM image of the surface is shown in figure 1(a). At the given coverage of ≈0.1 ML we observe single molecules adsorbed on the bare Cu substrate in agreement with previous results for other metal phthalocyanine molecules on Cu(1 0 0) [35, 36] and SnPc adsorbed on Ag(1 1 1) [20, 21]. Owing to the fact that the Sn atom in the center cavity is too large to fit into it, the otherwise planar phthalocyanine organic framework exhibits a shuttle-cock shape [37, 38]. This gives rise to two conformations with the Sn atom either pointing away from (Sn-up, dashed circle in figure 1(a)) or towards (Sn-down, solid circle in figure 1(a)) the surface. Owing to a height difference in between the two configurations, Sn-up appears higher than Sn-down by ≈0.5 Å[5]. We observed two different molecular orientations, which are rotated by ≈50° with respect to each other as indicated by solid lines in figure 1(a). Similar adsorption geometries were found for metal phthalocyanines on Ag(1 0 0) [39, 40] and Cu(1 0 0) [35, 41] surfaces.

A top-view of the calculated geometry of Sn-down on the Cu(1 0 0) surface is shown in figure 1(b). Examples of pyrrole (N_p) and azopyrrole (N_a) nitrogen atoms are indicated by arrows. The calculated angle of the molecular lobes with respect to the [1 1 0] direction of the substrate is ±27°, in good agreement with the experimentally observed orientations. Our calculations yield an adsorption energy of 6.3 eV for Sn-down molecules with the Sn adsorbed at a hollow site of the Cu mesh. This energy is a little larger than for Sn-down on Ag(1 1 1), where 5.98 eV and 5.28 eV were obtained with cluster and periodic DFT calculations including dispersion interactions, respectively [38]. Compared to the hollow site, adsorption to top positions of Cu(1 0 0) is unstable, and the molecule always relaxes to back to the hollow site. We find that the electron density is decreased between the Sn atom and the surface, whereas an increase occurs underneath the molecular π orbitals (see discussion of figure 3(c) below). We therefore conclude that the π orbitals contribute significantly to the adsorption on Cu(1 0 0) in addition to the binding of

[5] The apparent height difference varied with the applied sample voltage V.

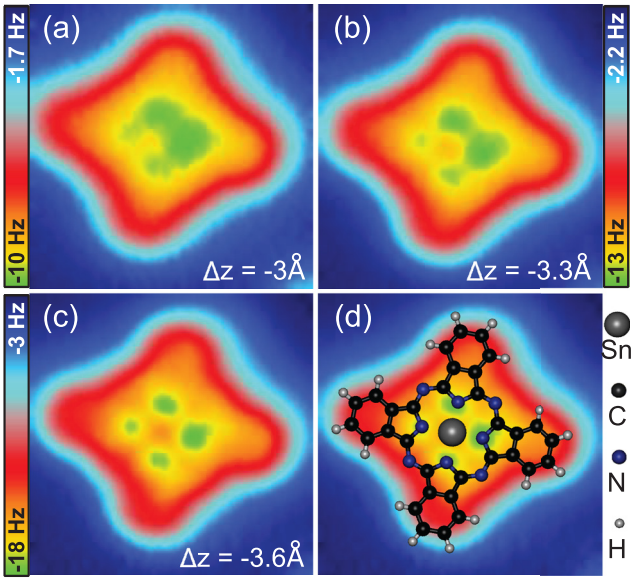

Figure 2. Constant-height frequency-shift images of Sn-down $(2\,\mathrm{nm})^2$. The tip oscillation amplitude was 1 Å for all images. $\Delta z = 0$ pm corresponds to the tip-molecule distance defined by current feedback parameters $V = -200$ mV and $I = 20$ pA over the molecular center. From this distance, the tip was brought closer to the surface by Δz as indicated in the images. (d) The image of (c) with the molecular structure overlaid. Most negative frequency shift is observed at N_p atoms.

the Sn to the surface. This is different from the adsorption of Sn-down on Ag(1 1 1) which binds mostly through a covalent bond of the Sn atom to the substrate [38]. The strength of the molecular binding with the Cu surface follows the general trend of significantly increased reactivity of Cu compared to other coinage surfaces, i.e. the (1 1 0), (1 0 0), and (1 1 1) surfaces of Cu, Ag, and Au [42].

3.2. Interaction between the tip and the molecule

The interaction between a Sn-down molecule and the tip was characterised by means of constant-height frequency-shift (Δf) maps (figure 2). Current feedback was disabled at a setpoint $V = -200$ mV and $I = 20$ pA and subsequently the tip was brought closer to the surface by the offsets indicated in panels (a) to (c). At large distance (figure 2(a)) the Sn-down molecule gives rise to a more negative Δf around the molecular center. This is due to van der Waals interaction and does not yield submolecular information. When the tip is brought closer by 60 pm (figure 2(c)), distinct areas of most negative Δf are observed above the N_p atoms. Within a lateral distance of only 4 Å, Δf changes from -15 Hz to -18 Hz and back. An overlay of the calculated molecular structure in figure 2(d) highlights the agreement of the N_p atom positions with the described features. Δf differs by ≈ 3 Hz between N_p and N_a indicating that the N atoms are not equivalent regarding the interaction with a metallic tip. We note that the slight asymmetry in all the images stems from a small tilt of the plane of tip motion with respect to the molecular plane. Constant-height Δf maps taken on molecules in the Sn-up state are dominated by the protruding Sn atom and do not show submolecular contrast.

All images in figure 2 were taken in a regime where a reduction of the tip-molecule distance leads to a more negative Δf, i.e. Pauli repulsion does not play a dominant role in the image contrast. This is different from previous works, which showed submolecular resolution close to the onset of Pauli repulsion, where Δf is most negative [2, 43]. Recently it was shown that the oxygen atoms in mercaptobenzoic acid molecule can be resolved in AFM images using a metallic tip in the attractive interaction regime [44]. In that case, electrostatic and, in particular, covalent contributions to the force were invoked along with relaxations of oxygen atoms towards the tip.

3.3. Discussion of the AFM contrast

Below, possible reasons of the submolecular contrast in the AFM images are discussed. Metallic tips have a permanent dipole moment pointing towards the surface [13, 45–47]. For a tetrahedral model tip consisting of 10 Cu-atoms on a copper slab we calculate a dipole moment of -2.6 D, in good agreement to previous results [12, 14, 45, 46]. Through this dipole, the tip should be sensitive to charge imbalances within the SnPc molecule. However, a Bader charge analysis [33] (figure 3(a)) shows that both N_p and N_a atoms are charged with ≈ -1.1 electrons each. Therefore, the tip dipole cannot explain a contrast that is only observed at N_p.

The net charge transfer from the surface to the molecule is roughly 1.8 electrons. An analysis of the electron density difference is shown in figure 3(b) revealing an electron transfer from the Sn to the four nearest Cu atoms around the hollow position. This indicates the formation of a polar covalent bond between Sn and the surface, as also suggested for Sn-down on Ag(1 1 1) [38]. In addition we find an increased electron density in the π orbitals nearest to the surface, which is not present on Ag(1 1 1). This shows that the π orbitals play an important role in the electron transfer here and not only the bond between the Sn atom and the surface as it was observed for Sn-down on Ag(1 1 1) [14, 38]

Figure 3(c) depicts a side-view of calculated adsorption geometry. We find that the N_p atoms are further away from the molecular plane (defined by the benzene rings) by $\sim$35 pm compared to N_a atoms, which lie within the molecular plane. The reason for this is that although the Sn-N_p bonds favour a flatter configuration in the isolated molecule [38], the bond formation with the surface pulls the molecule closer to it. Therefore, the N_p atoms are forced to move up to keep a suitable distance to the Sn. The protrusion of N_p atoms is thereby caused by the Sn atom below the molecular plane. Thus, we expect this deformation not to be present in the Sn-up state. The distance between the top Cu layer and the molecular plane and is $\sim$2.3 Å and just 1.9 Å for the Sn atom, which is both smaller than for SnPc on Ag(1 1 1) [14, 48, 49] or various transition metal Pc molecules on Ag(1 0 0) [40]. We ascribe the increased binding manifesting in the electron transfer to the π orbitals, the lower adsorption distance as well as the displacement of N_p to the stronger reactivity of the Cu(1 0 0) surface.

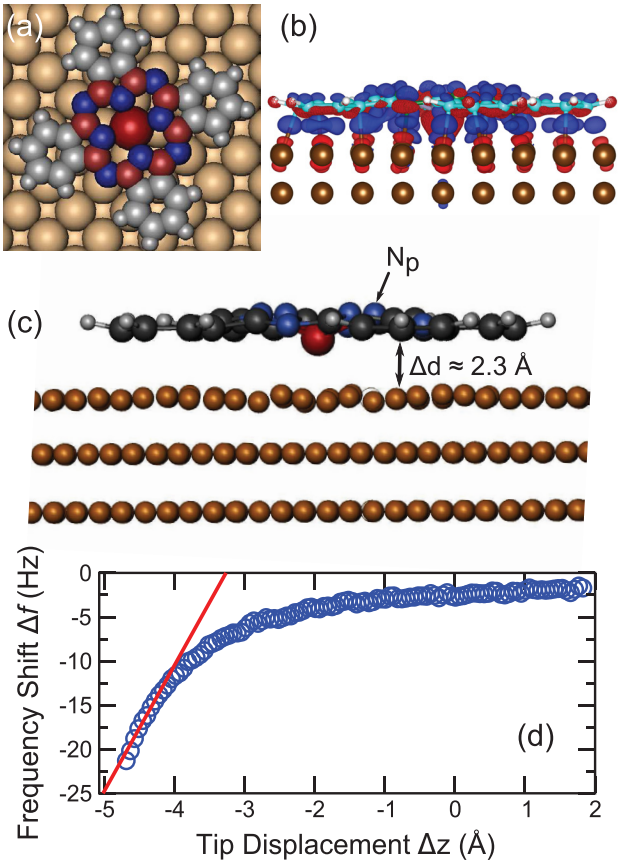

Figure 3. (a) Calculated net charges ascribed to the individual atoms of the molecule. Positive and negative charges are plotted in red and blue, respectively. (b) Charge difference plot for Sn-down on Cu(1 0 0) (side view) with red and blue showing a decreased and increased electron density, respectively. (c) Side-view of the calculated Sn-down configuration. N_p atoms (arrow) are further away from the top Cu layer by ∼35 pm compared to the molecular plane. Mean distance Δd between the top Cu layer and the molecular plane is ∼2.3 Å. (d) Exemplary frequency shift Δf versus tip displacement Δz curve recorded over N_p. The slope at −15 Hz is $\sim 7\frac{\text{pm}}{\text{Hz}}$ (red line).

As AFM with metallic tips is sensitive to the electron density, an increased attractive force is expected above the protruding N_p atoms at a fixed distance of the tip with respect the molecular plane. This corresponds to a more negative Δf. Figure 3(d) shows the measured frequency shift versus distance $\Delta f(z)$ recorded above a N_p atom. At $\Delta f = -15$ Hz, the tip-molecule distance at which the images in figure 2 were acquired, the slope of $\Delta f(z)$ is $\approx 7\frac{\text{pm}}{\text{Hz}}$[6]. Using this slope a height difference of 18 to 48 pm is estimated from the Δf difference (for different tips) between the molecular plane and the N_p positions. This range matches the calculated height difference of 35 pm. We therefore suggest that the distinct features in figure 2(c) are mainly caused by the protruding N_p atoms. Relaxations of the tip and the N_p atoms are expected to be small because the AFM images were acquired at large tip-sample distances.

[6] For different tips, this value varies from 6–16 $\frac{\text{pm}}{\text{Hz}}$ at the relevant Δf range, presumably due to the influence of long-range forces.

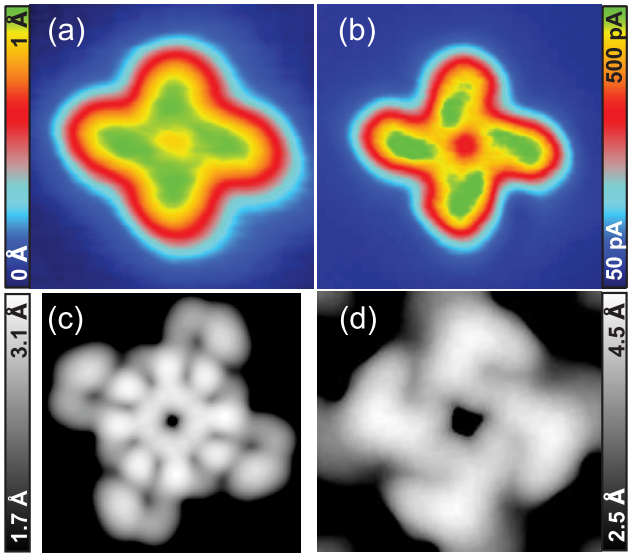

Figure 4. (a) Constant-current and (b) constant-height STM images of a Sn-down molecule ($V = 200$ mV, $(2.2\,\text{nm})^2$) exhibit chiral motifs. Current contours calculated for (c) $V = 100$ mV and (c) $V = -100$ mV reproduce the chirality.

3.4. Chirality of the electronic structure

For a discussion of the electronic structure close to the Fermi energy, figures 4(a) and (b) show constant-current and constant-height STM images. While the AFM image (figure 2(c)) shows contrast at N_p atoms, no such effect is discernible in the STM data. Rather, a chirality of the four lobes of the Sn-down molecule is observed. This chirality is particularly obvious in the constant-height data (figure 4(b)).

While SnPc is achiral in gas phase [19], a handedness was observed for adsorbed Pc molecules on Ag(1 0 0) [39, 40] and Cu(1 0 0) [35, 50]. The chirality was characterised as being due to an asymmetric charge transfer between the molecule and the substrate, that involves hardly any distortion of the molecular structure [39]. This interpretation is consistent with our data, namely achiral AFM maps and chiral STM images. In addition, calculated contour plots of the electron density near the Fermi level (figures 4(c) and (d)) clearly show a chirality of the molecular lobes. When states at larger energies are included ($V \geqslant 0.5$ V or $V \leqslant -0.2$ V) the chirality is absent.

4. Conclusion

Sn-phthalocyanine molecules adsorbed on Cu(1 0 0) were investigated with scanning tunnelling and atomic force microscopy. Submolecularly resolved AFM images recorded with metal tips exhibit distinct attractive features at pyrrole nitrogen atoms. Density functional theory results show that electrostatic forces are negligible. Rather, the strong interaction between the phenyl rings of SnPc and the Cu substrate deforms the molecule and causes the N_p atoms to protrude by 35 pm over the molecular plane. STM images reveal chirality of the molecular lobes in agreement with our DFT calculations. Our work shows that combined scanning tunnelling and atomic force microscopy can be used to distinguish between structural and electronic effects within a single molecule.

Acknowledgments

Support through SFB 677 of Deutsche Forschungsgemeinschaft is gratefully acknowledged. ASF has been supported by the Academy of Finland through its Centres of Excellence Program project no. 915804 and EU project PAMS (contract no. 610446), and acknowledges use of the CSC, Helsinki for computational resources.

References

[1] Tersoff J and Hamann D R 1985 *Phys. Rev.* B **31** 805–13
[2] Gross L, Mohn F, Moll N, Liljeroth P and Meyer G 2009 *Science* **325** 1110–4
[3] Gross L, Mohn F, Moll N, Meyer G, Ebel R, Abdel-Mageed W M and Jaspars M 2010 *Nat. Chem.* **2** 821–5
[4] Oteyza D G D *et al* 2013 *Science* **340** 1434–7
[5] Ernst K H, Baumann S, Lutz C P, Seibel J, Zoppi L and Heinrich A J 2015 *Nano Lett.* **15** 5388–92
[6] Moll N *et al* 2014 *Nano Lett.* **14** 6127–31
[7] Neu M, Moll N, Gross L, Meyer G, Giessibl F J and Repp J 2014 *Phys. Rev.* B **89** 205407
[8] Hämäläinen S K, van der Heijden N, van der Lit J, den Hartog S, Liljeroth P and Swart I 2014 *Phys. Rev. Lett.* **113** 186102
[9] Hapala P, Kichin G, Wagner C, Tautz F S, Temirov R and Jelínek P 2014 *Phys. Rev.* B **90** 085421
[10] Hauptmann N, González C, Mohn F, Gross L, Meyer G and Berndt R 2015 *Nanotechnology* **26** 445703
[11] Mönig H, Hermoso D R, Díaz Arado O, Todorović M, Timmer A, Schüer S, Langewisch G, Pérez R and Fuchs H 2016 *ACS Nano* **10** 1201–9
[12] Schwarz A, Köhler A, Grenz J and Wiesendanger R 2014 *Appl. Phys. Lett.* **105** 011606
[13] Schneiderbauer M, Emmrich M, Weymouth A J and Giessibl F J 2014 *Phys. Rev. Lett.* **112** 166102
[14] Caffrey N M, Buchmann K, Hauptmann N, Lazo C, Ferriani P, Heinze S and Berndt R 2015 *Nano Lett.* **15** 5156–60
[15] van der Lit J, Di Cicco F, Hapala P, Jelínek P and Swart I 2016 *Phys. Rev. Lett.* **116** 096102
[16] Ellner M, Pavliček N, Pou P, Schuler B, Moll N, Meyer G, Gross L and Peréz R 2016 *Nano Lett.* **16** 1974–80
[17] Woods L M, Dalvit D A R, Tkatchenko A, Rodriguez-Lopez P, Rodriguez A W and Podgornik R 2016 *Rev. Mod. Phys.* **88** 045003
[18] Kawai S, Foster A S, Björkman T, Nowakowska S, Björk J, Canova F F, Gade L H, Jung T A and Meyer E 2016 *Nat. Commun.* **7** 11559
[19] Torre G D L, Claessens C G and Torres T 2007 *Chem. Commun.* 2000–15
[20] Wang Y, Kröger J, Berndt R and Hofer W 2009 *Angew. Chem. Int. Ed.* **48** 1261–5
[21] Wang Y, Wu K, Kröger J and Berndt R 2012 *AIP Adv.* **2** 041402
[22] Lackinger M and Hietschold M 2002 *Surf. Sci.* **520** L619–24
[23] Toader M and Hietschold M 2011 *J. Phys. Chem.* C **115** 3099–105
[24] Toader M and Hietschold M 2011 *J. Phys. Chem.* C **115** 12494–500
[25] CreaTec Fischer & Co. GmbH www.createc.de
[26] Giessibl F J 1998 *Appl. Phys. Lett.* **73** 3956–8
[27] Kresse G and Furthmüller J 1996 *Comput. Mater. Sci.* **6** 15–50
[28] Kresse G and Furthmüller J 1996 *Phys. Rev.* B **54** 11169–86
[29] Klimeš J, Bowler D R and Michaelides A 2010 *J. Phys.: Condens. Matter* **22** 022201
[30] Klimeš J, Bowler D R and Michaelides A 2011 *Phys. Rev.* B **83** 195131
[31] Börkman T, Gulans A, Krasheninnikov A V and Nieminen R M 2012 *Phys. Rev. Lett.* **108** 235502
[32] Blöchl P E 1994 *Phys. Rev.* B **50** 17953–79
[33] Tang W, Sanville E and Henkelman G 2009 *J. Phys.: Condens. Matter* **21** 084204
[34] Vanpoucke D E P and Brocks G 2008 *Phys. Rev.* B **77** 241308
[35] Chen F *et al* 2012 *Appl. Phys. Lett.* **100** 081602
[36] Rehman R A, Dou W, Qian H, Mao H, Floether F, Zhang H, Li H, He P and Bao S 2012 *Surf. Sci.* **606** 1749–54
[37] Day P, Wang Z and Pachter R 1998 *J. Mol. Struct. Theochem.* **455** 33–50
[38] Baran J D and Larsson J A 2012 *J. Phys. Chem.* C **116** 9487–97
[39] Mugarza A, Lorente N, Ordejón P, Krull C, Stepanow S, Bocquet M L, Fraxedas J, Ceballos G and Gambardella P 2010 *Phys. Rev. Lett.* **105** 115702
[40] Mugarza A, Robles R, Krull C, Korytár R, Lorente N and Gambardella P 2012 *Phys. Rev.* B **85** 155437
[41] Chang S H, Kuck S, Brede J, Lichtenstein L, Hoffmann G and Wiesendanger R 2008 *Phys. Rev.* B **78** 233409
[42] Jiang Y, Yang S, Li S and Liu W 2016 *Sci. Rep.* **6** 39529
[43] Gross L, Mohn F, Moll N, Schuler B, Criado A, Guitian E, Pena D, Gourdon A and Meyer G 2012 *Science* **337** 1326–9
[44] Hauptmann N, Robles R, Abufager P, Lorente N and Berndt R 2016 *J. Phys. Chem. Lett.* **7** 1984–90
[45] Teobaldi G, Lämmle K, Trevethan T, Watkins M, Schwarz A, Wiesendanger R and Shluger A L 2011 *Phys. Rev. Lett.* **106** 216102
[46] Gao D Z, Grenz J, Watkins M B, Federici Canova F, Schwarz A, Wiesendanger R and Shluger A L 2014 *ACS Nano* **8** 5339–51
[47] Gross L, Schuler B, Mohn F, Moll N, Pavliček N, Steurer W, Scivetti I, Kotsis K, Persson M and Meyer G 2014 *Phys. Rev.* B **90** 155455
[48] Stadler C, Hansen S, Pollinger F, Kumpf C, Umbach E, Lee T L and Zegenhagen J 2006 *Phys. Rev.* B **74** 035404
[49] Greif M, Castiglioni L, Seitsonen A, Roth S, Osterwalder J and Hengsberger M 2013 *Phys. Rev.* B **87** 085429
[50] Cai Y, Xu S, Qiao X, Wang L, Liu Y, Wang T and Xu X 2015 *Phys. Chem. Chem. Phys.* **17** 23651–6